Abdominal Radiology (2019) 44:1237–1245
https://doi.org/10.1007/s00261-018-1865-9

SPECIAL SECTION: DISTINGUISHED PAPERS FROM JSAR

Comparison of characteristic computed tomographic findings of gastrointestinal and non-gastrointestinal stromal tumors in the small intestine

Akitoshi Inoue[1] · Shinichi Ota[1] · Shigetaka Sato[1] · Norihisa Nitta[1] · Tomoharu Shimizu[2] · Hiromichi Sonoda[2] · Masaji Tani[2] · Hiromitsu Ban[3] · Osamu Inatomi[3] · Akira Ando[3] · Ryoji Kushima[4] · Kiyoshi Murata[1]

Published online: 1 January 2019
© Springer Science+Business Media, LLC, part of Springer Nature 2019

Abstract

Purpose We aimed to reveal specific findings of gastrointestinal stromal tumors (GISTs) in the small intestine on contrast-enhanced computed tomography (CT) by comparing GISTs with non-GISTs.

Methods We enrolled 28 patients with 39 GISTs and 20 patients with 22 non-GISTs who underwent enterectomy with a preoperative diagnosis of small intestinal tumor. All lesions were diagnosed by histopathological examination. Two radiologists independently evaluated internal homogeneity, growth pattern, calcification, intratumoral hemorrhage, degeneration, ulceration, and lymphadenopathy and measured the maximum diameter of the tumor and contrast-enhanced CT (CECT) value of the solid portion as well as the diameter and CT value of the feeding artery and drainage vein on CECT in the arterial and venous phases.

Results Intratumoral hemorrhage was seen in 15.4% and 25.6% of GISTs and in 0% and 0% of non-GISTs ($p=0.079$ and 0.010), with good interobserver agreement ($\kappa=0.715$). The drainage vein diameter correlated well with the maximum diameter of the tumor ($r=0.744$, $p<0.001$). The CT value of the solid tumor part in the arterial and venous phases ($p<0.01$) and the CT value of the drainage vein in the arterial phase ($p<0.05$) were higher for GISTs than for non-GISTs ($p<0.01$).

Conclusions Strong parenchymal enhancement with the peak in the arterial phase and the CT value of the drainage vein in the arterial phase was characteristics findings of GIST compared with non-GISTs. The diameter of the drainage vein was proportional to the maximum diameter of GISTs.

Keywords Gastrointestinal stromal tumor · Small intestine · Drainage vein · Computed tomography

Introduction

Gastrointestinal stromal tumors (GISTs) are the most common submucosal mesenchymal tumor of the alimentary tract. GISTs arise most commonly in the stomach (50–70%), followed by the jejunum and ileum (30–40%), duodenum (5%), colon (4%), and esophagus or appendix (1%), and they most commonly occur at ages 50s to 60s [1–3]. GISTs arise from Cajal interstitial cells, which are the pacemaker cells located at Auerbach's plexus of the alimentary tract [4]. GISTs are characterized by their expression of KIT (CD117), a tyrosine kinase growth factor receptor, which is important for distinguishing GISTs from other mesenchymal tumors, including leiomyoma, leiomyosarcoma, and Schwannoma [5]. The histopathological diagnosis by endoscopic biopsy is easily performed in the esophageal, gastric, and duodenal tracts, whereas it is more difficult and invasive for small

✉ Akitoshi Inoue
akino@belle.shiga-med.ac.jp

1 Department of Radiology, Shiga University of Medical Science, Seta, Tsukinowa-cho, Otsu City, Shiga 520-2192, Japan

2 Department of Surgery, Shiga University of Medical Science, Seta, Tsukinowa-cho, Otsu City, Shiga 520-2192, Japan

3 Department of Gastroenterology, Shiga University of Medical Science, Seta, Tsukinowa-cho, Otsu City, Shiga 520-2192, Japan

4 Department of Pathology, Shiga University of Medical Science, Seta, Tsukinowa-cho, Otsu City, Shiga 520-2192, Japan

intestinal tumors because enteroscopy requires sedation and a long procedure time of > 1 h and sometimes causes complications, such as aspiration pneumonia, bleeding, perforation, and pancreatitis [6].

Computed tomography (CT), especially CT enteroclysis (CTE), is helpful in the detection of small bowel neoplasms [7, 8]. Most GISTs detected by CTE are not malignant because CTE is able to depict the smaller GISTs that are not detected by conventional CT [9]. Detection of small intestinal tumors is a crucial role of CT. The treatment strategy should be determined after detection. Although most small intestinal tumors without metastasis should be surgically resected, the treatment strategy depends on the tumor and remote metastasis. GISTs with hepatic metastasis are treated with tyrosine kinase inhibitors; therefore, evaluation of tumor extension is the essential role of CT. Furthermore, differential diagnosis from the other submucosal tumors such as neurogenic tumors, neuroendocrine tumors, lymphomas, desmoids, metastatic tumors, and other rare mesenchymal tumors is desirable in small intestinal GISTs before treatment, because imaging diagnosis of metastatic small intestinal tumors is clinically significant as they are treated by chemotherapy depending on the primary lesion and malignant lymphoma is treated by chemotherapy, which does not require complete resection but rather en-block tissue sampling. Although typical lymphoma presents a bulky mass with homogeneous tumor with markedly high intensity on diffusion-weighted image and high accumulation of fluorodeoxyglucose on positron emission tomography, imaging spectrum of lymphomas is broad and some of them are difficult to diagnose with imaging. Multiphasic CT can be useful to differentiate among small bowel neoplasms on the basis of enhancement patterns [10]. Previous articles, however, have reported various imaging presentations of GISTs, such as calcification, intratumoral hemorrhage, and degeneration, and the tumor size and growth pattern are extremely variable [1, 11]. The purpose of this study was, therefore, to reveal specific findings of small intestinal GISTs on contrast-enhanced CT (CECT) by comparing GISTs with non-GISTs.

Materials and methods

This retrospective study was approved by our Institutional Review Board, and written informed consent was waived.

Patients

We enrolled consecutive 59 patients who underwent enterectomy with preoperative diagnosis of the small intestinal tumor at our institution between January 2007 and December 2016. Two patients who underwent only non-contrast CT and one patient with small lesion which was not depicted on CT were excluded and 56 patients (33 males, 23 females, mean age 61.2 years, age range 29–81 years) with 69 lesions were enrolled in this study. Of patients with GISTs, 28 patients with 39 lesions were diagnosed as having GISTs. Two patients had two simultaneous lesions, one patient had three simultaneous lesions, and one patient diagnosed as having familial GISTs had eight simultaneous lesions. Of the patients with non-GISTs, 28 patients with 30 lesions were diagnosed as having non-GISTs. The non-GISTs group consisted of 10 metastases, including lung cancer ($n = 5$), uterine sarcoma ($n = 2$), renal cell carcinoma (RCC, $n = 2$), and pharyngeal cancer ($n = 1$) and 1 patient with metastasis from lung cancer had 3 lesions, 6 malignant lymphomas, 5 primary adenocarcinomas, 1 neuroendocrine tumor, 1 desmoid tumor, 1 low-grade fibromyxoid sarcoma, 1 ectopic pancreas, 1 Schwannoma, 1 lipoma, 1 liposarcoma, 1 IgG4-related disease, and 1 Crohn's disease. One lipoma, 1 Crohn's disease, 1 IgG4-related disease, and 5 adenocarcinomas were omitted from non-GIST group because these lesions are relatively easily distinguish from GISTs, consequently 20 patients with 22 lesions were enrolled in non-GIST group (Table 1).

CT examinations

CT examinations were performed on three scanners: a 320-row multidetector (MDCT) (Aquilion ONE; Canon Medical Systems, Otawara, Japan), a 64-row MDCT (Aquilion 64; Canon Medical Systems, Otawara, Japan), and a 16-row MDCT (SOMATOM SENSATION CA; Siemens, Germany). Both non-contrast and CECT scans (arterial and venous phase) were performed. The scans were performed during breath holding while using the following parameters: 256–256 matrix, 320–380 mm FOV, 120 kVp, 270 mA or auto mA mode, and a section thickness interval of 5 mm. Intravenous administration of iodine contrast media was injected by using an automatic power injector. A total amount of 600 mg I/kg of iopamidol (Iopamiron 370 Bayer Yakuhin, Osaka, Japan or Oypalomin 370, Fuji Pharma,

Table 1 The details in non-GISTs group

Non-GISTs group	
Metastatic tumor	10
Malignant lymphoma	6
Neuroendocrine tumor	1
Desmoid tumor	1
Low-grade fibromyxoid sarcoma	1
Ectopic pancreas	1
Schwannoma	1
Liposarcoma	1
Total	22

Tokyo, Japan), iohexol (Omnipaque 300, Daiichi-Sankyo, Tokyo, Japan or Ioverin 350, Teva Takeda Pharma, Nagoya, Japan), or iomeprol (Iomeron 350; Eisai, Tokyo, Japan) was injected at a rate depending on the patient's body weight. CT scans were obtained pre-contrast and during both the early 40-s delay (arterial) phase and 100-s delay (venous) phase.

Image analysis

Two abdominal radiologists (A.I. and S.O. with 12 and 24 years of experience reading gastrointestinal images, respectively) who knew only that the patients had small bowel tumors and were blinded to the pathological diagnosis independently reviewed the unenhanced and CECT images.

Qualitative analysis

We reviewed axial images with 5 mm thickness and visually classified (a) internal homogeneity of the tumor in the venous phase of CECT into homogeneous or heterogeneous and (b) growth pattern of the tumor into endophytic, exophytic, or intramural (Fig. 1). Moreover, we visually evaluated the presence or absence of (c) calcification: high-density area on non-contrast CT, (d) intratumoral hemorrhage: slightly high-density area in the tumor on non-contrast CT, (e) degeneration: no enhancement region in the tumor on CECT in the venous phase, (f) ulceration: intratumoral air density connected to the gastrointestinal lumen, (g) lymphadenopathy: swelled lymph node in the mesentery of > 5 mm, and (h) early venous return: enhancement in the drainage vein equal to that of the artery on CECT in the arterial phase (Fig. 2).

Quantitative analysis

We measured the (A) maximum diameter of the tumor on axial images, (B) CT value of the solid portion of the tumor on unenhanced CT and CECT in the arterial and venous phases, (C) diameter of the feeding artery and CT value on CECT in the arterial and venous phase, and (D) diameter of the drainage vein and CT value on CECT in the arterial and venous phase.

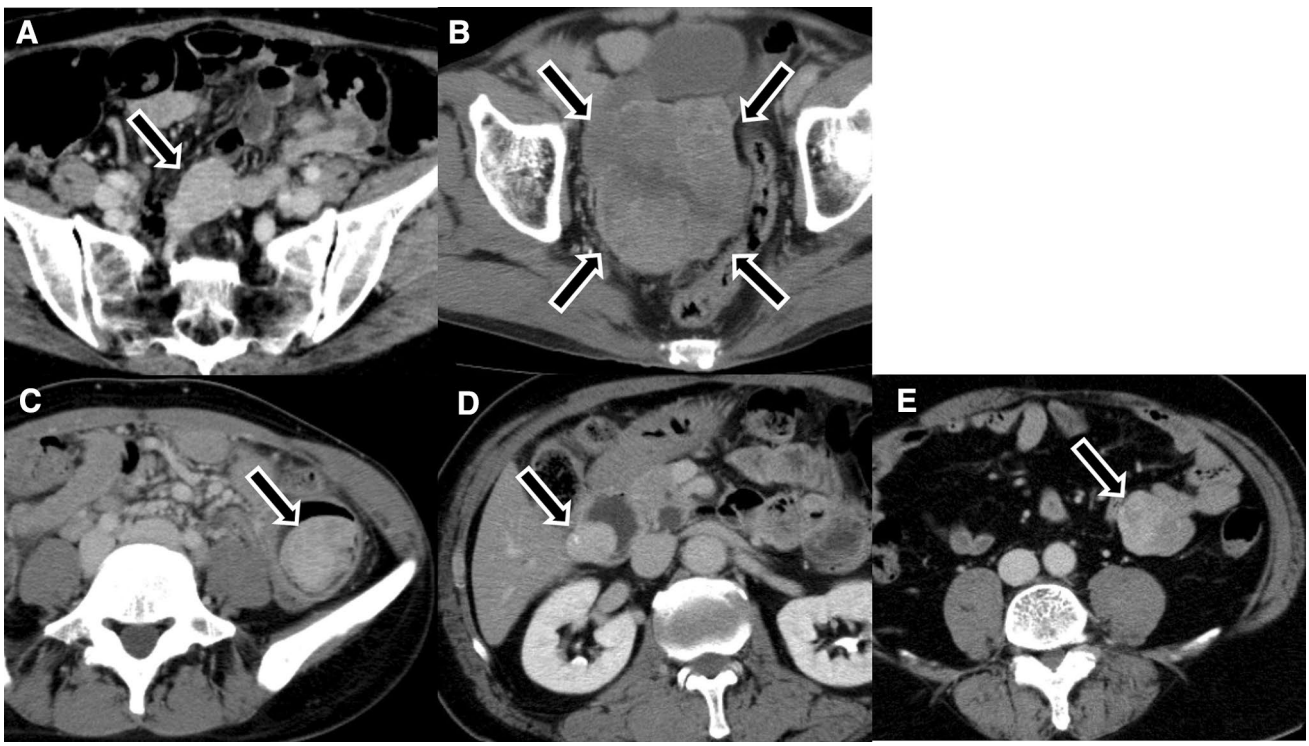

Fig. 1 Qualitative analysis regarding internal homogeneity and growth pattern. **a** Homogeneous: a 59-year-old female with a small intestinal gastrointestinal stromal tumor (GIST) that is homogeneous on contrast-enhanced computed tomography (CT) in the equilibrium phase (arrow). **b** Heterogeneous: a 64-year-old male with a small intestinal GIST presenting a heterogeneous pattern on contrast-enhanced CT in the equilibrium phase (arrow). **c** Endophytic growth pattern: a 43-year-old female with a small intestinal GIST growing into the lumen of the small intestine. **d** Intramural growth pattern: a 78-year-old female with a small intestinal GIST growing concentrically against the small intestinal wall. **e** Exophytic growth pattern: a 53-year-old male with a small intestinal GIST growing outside the small intestinal lumen

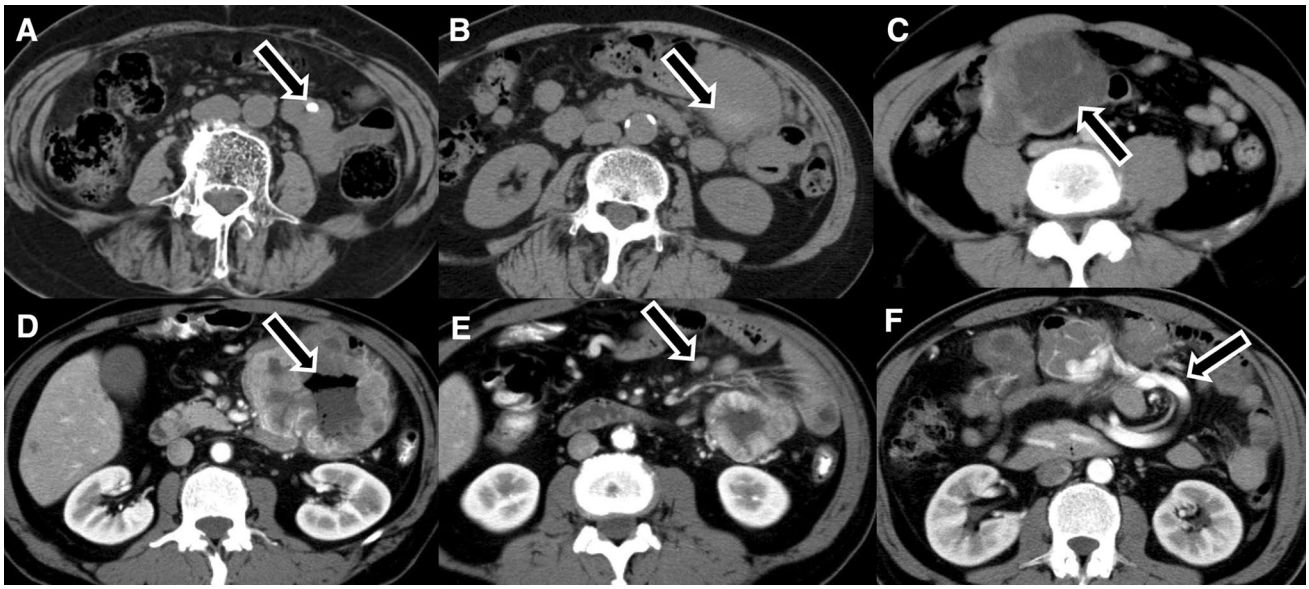

Fig. 2 Qualitative analysis of representative findings. **a** Calcification: a 73-year-old female with a small intestinal gastrointestinal stromal tumor (GIST) containing nodular calcification on non-contrast computed tomography (CT) (arrow). **b** Intratumoral hemorrhage: a 67-year-old female with a small intestinal GIST, including a slight high-density area on non-contrast CT (arrow). **c** Degeneration: a 54-year-old male with a small intestinal GIST with a non-enhanced component (arrow). **d**, **e** Ulceration and lymphadenopathy: a 67-year-old male with a small intestinal GIST presenting air density in the tumor (**d** arrow) and swelled lymph nodes in the mesentery (**e** arrow). **f** Early venous return: a 56-year-old male with a small intestinal GIST on enhancement in the dilated drainage vein (arrow)

Statistical analysis

Qualitative and quantitative analyses between the GISTs and non-GISTs groups were assessed by using Fisher's exact test and Student's *t* test, respectively. *p* values of < 0.05 were considered as indicative of statistical significance. Interobserver agreement in qualitative analysis was assessed by using κ statistics and was categorized as poor (< 0.20), fair (0.21–0.40), moderate (0.41–0.60), good (0.61–0.80), and excellent (0.81–1.00). Statistical tests were performed by using SPSS statistics 22 (IBM, Chicago, IL). The correlations between the diameter of the drainage vein and maximum diameter and contrast enhancement were assessed by Pearson's correlation analysis.

Results

In the qualitative analysis, intratumoral hemorrhage was seen only in the GISTs group and there was significant difference by one observer ($p = 0.010$; Table 2). There were no significant differences in the other evaluated items between the two groups. In the GISTs group, lymphadenopathy was observed with ulceration (Fig. 2d, e). Early venous return was frequently observed in the GISTs group compared to the non-GISTs group. In the non-GISTs group, early venous return was confirmed in metastasis from clear cell RCC ($n = 2$, Fig. 3), malignant lymphoma ($n = 1$), and desmoid tumor ($n = 1$, Fig. 4) by both observers.

In the quantitative analysis, the CT value of the solid part of the tumor on CECT in the arterial and venous phases, and the CT value of the drainage vein in the arterial phase in the GISTs group were higher than those in the non-GISTs group (Table 3). The peak of enhancement was confirmed in the arterial phase in GISTs and non-GISTs group (Fig. 5). The drainage vein diameter was most correlated with the maximum diameter (Figs. 6, 7).

Discussion

We analyzed qualitative and quantitative CT findings of the small intestinal tumor to distinguish GISTs with non-GISTs. In the qualitative analysis, intratumoral hemorrhage and early venous return were observed more frequently in GISTs than in non-GISTs, with good and excellent interobserver agreement, respectively, however, there was no significant difference in early venous return between both groups. In the quantitative analysis, the GISTs showed stronger enhancement in the arterial and venous phases than in non-GISTs. The peak of enhancement was also observed in the arterial phase in both GISTs and non-GISTs. CT value of the drainage vein was higher at arterial phase in GISTs than in non-GISTs. Additionally, the drainage vein diameter correlated with the GIST diameter associated with early venous return.

Table 2 The results of qualitative analysis

	Observer 1			Observer 2			κ Values
	GISTs	Non-GISTs	p values	GISTs	Non-GISTs	p values	
Homogeneous	38.5% (15/39)	54.5% (12/22)		25.6% (10/39)	31.8% (7/22)		
Heterogeneous	61.5% (24/39)	45.5% (10/22)	0.287	74.4% (29/39)	68.2% (15/22)	0.767	0.516
Endophytic	7.7% (3/39)	31.8% (7/22)		5.1% (2/39)	36.4% (8/22)		
Intramural	10.3% (4/39)	34.6% (8/22)		38.5% (15/39)	22.7% (5/22)		
Exophytic	79.5% (31/39)	31.8% (722)	N/A	53.8% (21/39)	40.9% (9/22)	N/A	0.384
Calcification	10.3% (4/39)	0% (0/30)	0.287	12.8% (5/39)	0% (0/22)	0.149	0.880
Intratumoral hemorrhage	15.4% (6/39)	0% (0/30)	0.079	25.6% (10/39)	0% (0/22)	0.010*	0.715
Degeneration	28.2% (11/39)	13.6% (3/22)	0.225	43.6% (17/39)	18.2% (4/22)	0.054	0.645
Ulceration	12.8% (5/39)	4.5% (1/22)	0.404	12.8% (5/39)	4.5% (1/22)	0.404	1.000
Lymphadenopathy	7.7% (3/39)	22.7% (5/22)	0.124	10.3% (4/39)	27.3% (6/22)	0.147	0.480
Early venous return	43.5% (17/39)	18.2% (4/22)	0.054	46.2% (18/39)	18.2% (4/22)	0.051	0.963

Significant difference (*$p < 0.05$, **$p < 0.01$)

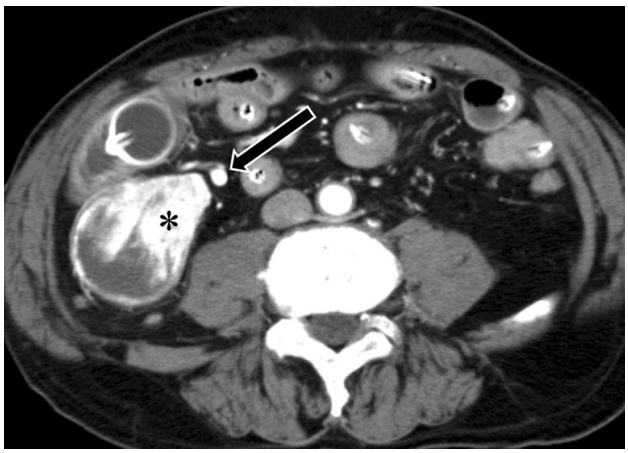

Fig. 3 Metastasis caused by renal cell carcinoma. A 71-year-old male had undergone right nephrectomy because of renal clear cell carcinoma 5 years earlier. The tumor shows extremely strong enhancement (asterisk), and early venous return in the dilated drainage vein (arrow) is observed in the small intestine

Modified Fletcher classification and Miettinen classification known as pathological risk-stratification of GISTs are determined by tumor size, mitosis, location, and presence or absence of rupture [12–14]. A previous article reported that tumor size, internal necrosis, internal air of enteric contrast, and ulceration on CT were associated with high-grade or malignant GISTs [9]. These findings were not helpful to distinguish GISTs from non-GISTs in this study. Enlarged vessels feeding or draining the mass also indicated high-risk GISTs as well as large size in previous article [15]. Our result showed that the diameter of drainage vein was directly proportional to the maximum diameter of the tumor, which indicated the confounding between the drainage vein and tumor size. Increasing venous return in large-sized GISTs seems to be natural because vascular bed and shunt is proportional to the tumor volume. We considered that the enlarged drainage vein may not be independent item to predict high-risk GIST.

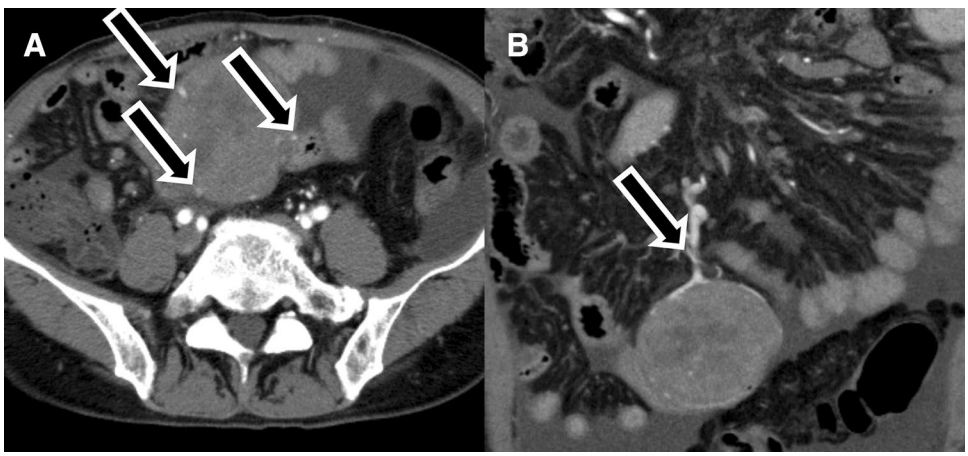

Fig. 4 Desmoid. A 64-year-old male was observed with a the submucosal tumor in the small intestine in follow up study for liver cirrhosis. The vasculature is seen in the peripheral parenchyma of the tumor (**a** arrows). Many vasculature early venous return is observed in the drainage vein (**b** arrow)

Table 3 The results of quantitative analysis

	Observer 1			Observer 2		
	GISTs	Non-GISTs	*p* values	GISTs	Non-GISTs	*p* values
Maximum diameter (mm)	44.7 ± 35.6	32.4 ± 20.6	0.145	47.0 ± 35.3	39.1 ± 21.7	0.347
CT value of solid part						
Non-enhanced (HU)	36.8 ± 4.9	36.0 ± 7.9	0.158	35.0 ± 4.7	35.2 ± 9.0	0.503
Arterial phase (HU)	145.6 ± 54.0	96.7 ± 49.8	0.001**	136.1 ± 46.2	96.3 ± 50.4	0.003**
Venous phase (HU)	108.6 ± 32.7	83.2 ± 21.3	0.003**	100.9 ± 25.6	80.3 ± 22.0	0.003**
Feeding artery						
Diameter (mm)	2.1 ± 0.7	2.1 ± 0.6	0.721	2.5 ± 1.1	2.2 ± 0.5	0.420
Arterial phase (HU)	205.2 ± 79.4	169.2 ± 64.1	0.124	195.9 ± 75.2	154.4 ± 30.8	0.139
Venous phase (HU)	114.5 ± 36.4	103.9 ± 41.9	0.362	114.5 ± 30.0	87.4 ± 26.9	0.050
Drainage vein						
Diameter (mm)	4.1 ± 2.3	3.2 ± 0.8	0.208	3.6 ± 1.7	3.2 ± 0.7	0.560
Arterial phase (HU)	231.6 ± 66.6	171.5 ± 99.7	0.024*	246.8 ± 51.8	196.1 ± 69.2	0.015*
Venous phase (HU)	149.0 ± 36.0	140.1 ± 48.7	0.496	134.8 ± 21.8	136.3 ± 32.6	0.901

Significant difference (*$p < 0.05$, **$p < 0.01$)

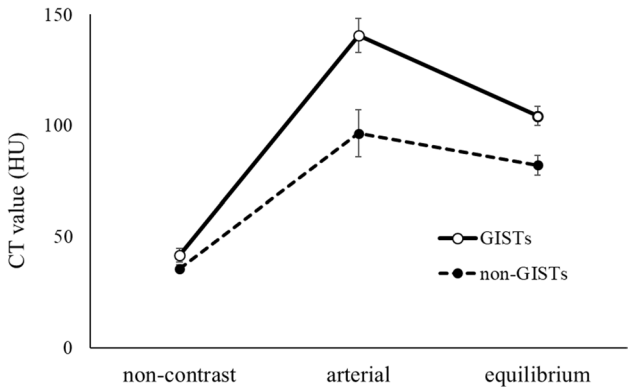

Fig. 5 Computed tomography (CT) values of a GIST and a non-GIST obtained in a dynamic study. The CT value of the GIST is higher than that of the non-GIST in the arterial and equilibrium phases with significant difference. The peak enhancement is seen in the arterial phase in both the GIST and non-GIST

In high-risk GISTs, peritoneal dissemination and liver metastasis are common [3, 16–19], although the incidence of lymph node metastasis is low and routine lymphadenectomy is not generally required [20]. In this study, lymphadenopathy was observed in a few cases of GISTs with ulceration; however, histopathological examination revealed no malignancy in the lymph nodes. We considered that reactive lymphadenopathy is often observed in GISTs with ulceration. These findings are compatible with those of previous reports, and it should be noted that lymphadenopathy is not rare when GISTs are accompanied by an ulceration.

Regarding intratumoral hemorrhage, 15.4% and 25.6% of the GISTs cases were observed by observers 1 and 2, respectively, but no cases of non-GISTs were observed although there is no significant difference by observer 1. In general, obvious and obscure gastrointestinal bleeding was a major complication of GISTs [1], and intraperitoneal rupture is also well known in GISTs [2]. Therefore, we speculated that intratumoral hemorrhage occurs frequently similar to gastrointestinal bleeding and intraperitoneal hemorrhage in GISTs, so we evaluated intratumoral hemorrhage in this study. We thought that intratumoral hemorrhage might be a characteristic finding of small intestinal GISTs, which is the first report of this finding and is a characteristic that should be helpful in the diagnosis of GISTs in the small intestine. We considered that intratumoral hemorrhage may lead to degeneration, calcification, and ulcer in case of penetration into the lumen.

Feeding artery and drainage vein are important to determine tumor origin [21]. We focused on characteristics of the feeding artery and drainage vein as well as parenchymal enhancement. In qualitative analysis, early venous return was seen more frequently in GISTs than in non-GISTs with high interobserver agreement, although there was no significant difference between GISTs and non-GISTs. On the other hand, in quantitative analysis, CT value of the drainage vein at arterial phase was higher in GISTs than that in non-GISTs. CT value of the drainage vein at arterial phase means venous return of iodine contrast media from the tumor which is affected by transit time of iodine contrast media through the tumor. In other words, it has the same meaning as early venous return. In this study, this feature so-called early venous return was detected not by qualitative analysis but by quantitative analysis because quantitative analysis seemed to be more sensitive than qualitative one. According to a previous article regarding duodenal GISTs by Cai et al., the blood supply from the superior and inferior pancreaticoduodenal artery and the presence of drainage directly into the portal venous trunk may be characteristic of duodenal GISTs [22].

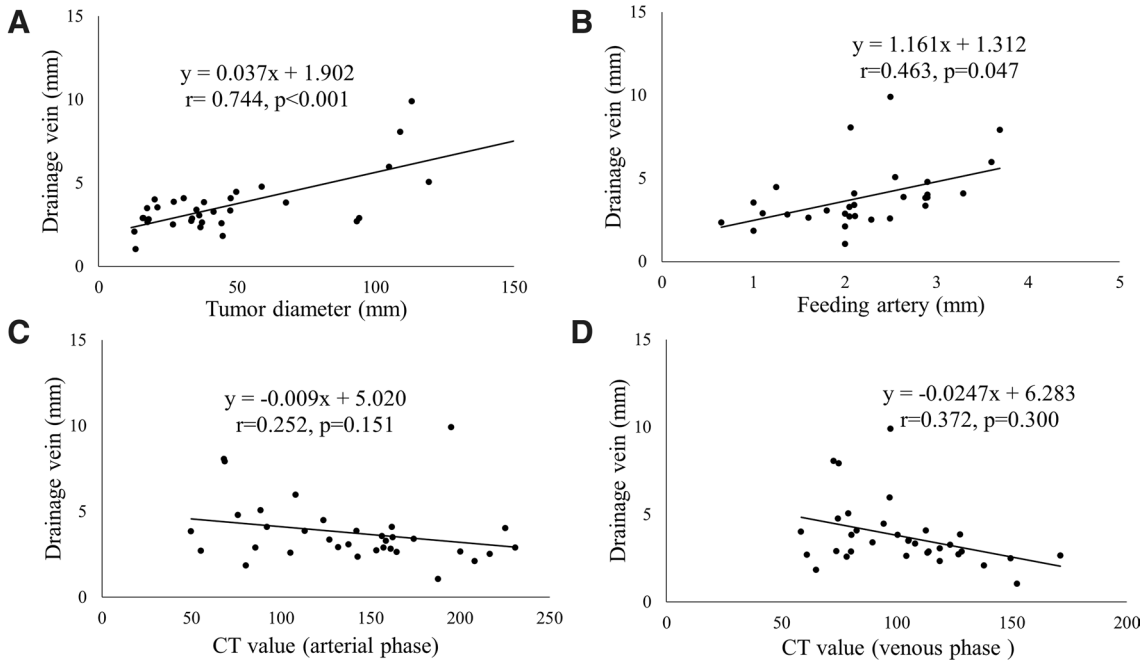

Fig. 6 The correlation between the diameter of the drainage vein and respective parameters. The diameter of the drainage vein was most correlated with the tumor diameter ($y = 0.037x + 1.902$, $r = 0.744$, $p < 0.001$)

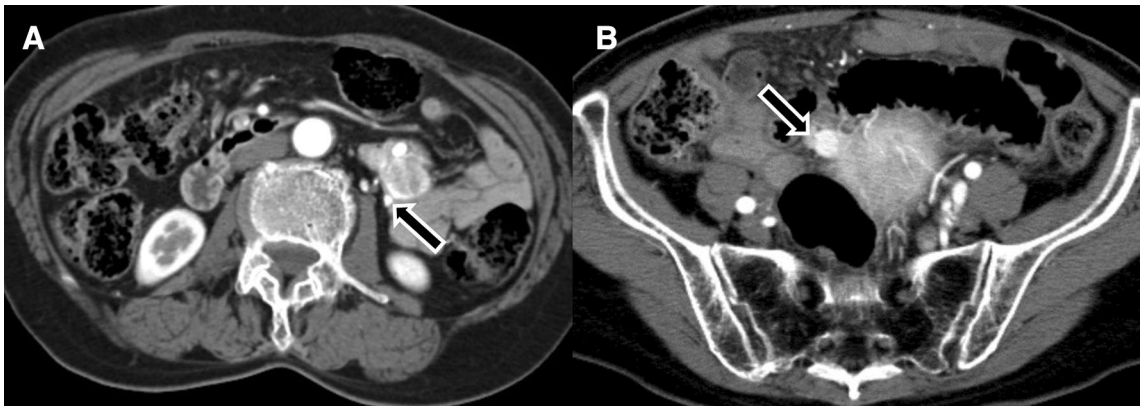

Fig. 7 The relationship between the diameter of the drainage vein and maximum diameter of the gastrointestinal stromal tumor (GIST). **a** A 73-year-old female showing a small intestinal GIST with a maximum diameter of 45.0 mm and a drainage vein diameter of 4.3 mm. **b** A 78-year-old female showing a small intestinal GIST with a maximum diameter of 113.0 mm and a drainage vein diameter of 9.9 mm

The finding that dilated veins near small intestinal GISTs were often observed in the arterial phase coincided with the characteristic finding of duodenal GISTs. Regarding the differential diagnosis between GISTs and non-GISTs, the diameters of the feeding artery and drainage vein were not helpful, but higher density of the drainage vein in the arterial phase could be useful for discrimination of GISTs from non-GISTs. This feature caused by one or both strong parenchymal enhancement meaning hypervascularity and large-diametered shunt by several marginal vessels as feeding artery and drainage vein in the GISTs. However, early venous return was also observed in non-GISTs, including metastases of clear cell RCC, malignant lymphoma, and desmoid tumor. Clear cell RCC is a highly dense tumor on CECT in the arterial phase and is caused by rich vascularity based on microvessel density proven by immunohistochemical examination using CD34 [23]. It seems reasonable that metastasis of clear cell RCC has same feature as primary lesion and their rich vascularity results in early venous return. Malignant lymphomas and desmoid tumors demonstrated early venous return, and however did not show as high density (80 and 73 HU, respectively) as metastasis

of clear cell RCCs (> 200 HU) in the arterial phase, which indicates they were not as hypervascular as clear cell RCCs. According to previous articles, lymphoma showed delayed enhancement pattern and desmoid showed mild to moderate enhancement due to collagen and myxoid element [10, 24]. Lymphoma and desmoid in this study presented vasculature in the peripheral parenchyma suggesting both the artery and vein and shunt between the artery and vein in peripheral of the tumor was considered. It should be noted that early venous return can be caused by not only parenchymal hyper vascularity but also extraparenchymal shunt.

As described earlier, early venous return is correlated with hypervascularity within the tumor. In this study, GISTs showed higher enhancement and stronger wash out than those in non-GISTs. An article regarding multiphasic dynamic CT by Shinya et al. showed that CT values could discriminate small intestinal neoplasms and concluded that GISTs and neuroendocrine tumors in the small intestine showed rapid enhancement followed by wash out in the venous phase, which is corroborated by our results [10]. Generally, enhancement of a tumor is dictated by the histological structure, such as vascular tissue and fibrous tissue, within the tumor. On the other hand, the cause and mechanism of early venous return in small intestinal tumors are not clear and has not been investigated, yet histopathologically, a shunt-like structure resembling an arteriovenous fistula could be one cause of early venous return in small intestinal GISTs, such as hepatic angiomyolipomas. The shunt between the arteriole and venule accelerates the intratumoral transit time of iodine contrast media. The reason for this is that multiphasic CT findings of the hepatic angiomyolipoma are similar to those of small intestinal GISTs in terms of marked enhancement and early venous return, and the cause of early venous return in hepatic angiomyolipoma is considered to be minimal arteriovenous shunt within the tumor on the basis of histopathological analysis [25, 26].

Our study has a few limitations. First, the CT scanners and protocol were not consistent because of the retrospective nature of the study. Second, our study population was relatively small because it was a single institute study, and the non-GISTs group included various diseases, such as metastases, adenocarcinomas, and malignant lymphomas. However, only one case of neuroendocrine tumor was enrolled. A previous article reported that neuroendocrine tumors as well as GISTs present a hypervascular pattern in the arterial phase with a washout in the venous phase on dynamic CT examinations [10]. Therefore, our results might have been different if many neuroendocrine tumors were present in the non-GISTs group. It is unclear if neuroendocrine tumors also show early venous return, so further investigation regarding CT findings is needed to distinguish GISTs when accompanied by neuroendocrine tumors. However, intratumoral hemorrhage, early venous return, and hypervascular parenchyma were found to be helpful findings for discrimination of GISTs from other small intestinal tumors except for neuroendocrine tumors.

In conclusion, GIST presented intratumoral hemorrhage more frequently than non-GIST. Strong parenchymal enhancement with the peak in the arterial phase was characteristic finding of GISTs. CT value of the drainage vein in the arterial phase presenting accelerated the intratumoral transit time of iodine contrast was higher in GISTs than that of non-GISTs and the diameter of the drainage vein was proportional to the maximum diameter of the GIST. These features enable us to distinguish GISTs from non-GISTs; however, the diameter and CT value of the feeding artery were not significantly different between GISTs and non-GISTs. Recognition of enhancement of tumor parenchyma and drainage vein can help in the interpretation of histological constructs such as vascularity and shunt.

Acknowledgements The authors would like to thank Enago (www.enago.jp) for the English language review.

Compliance with ethical standards

Conflict of interest No potential conflict of interest was reported by the authors.

References

1. Scola D, Bahoura L, Copelan A, et al (2017) Getting the GIST: a pictorial review of the various patterns of presentation of gastrointestinal stromal tumors on imaging. Abdom Radiol 42:1350–1364. https://doi.org/10.1007/s00261-016-1025-z
2. Baheti AD, Shinagare AB, O'Neill AC, et al (2015) MDCT and clinicopathological features of small bowel gastrointestinal stromal tumours in 102 patients: A single institute experience. Br J Radiol 88. https://doi.org/10.1259/bjr.20150085
3. Kochhar R, Manoharan P, Leahy M, Taylor MB (2010) Imaging in gastrointestinal stromal tumours: Current status and future directions. Clin Radiol 65:584–592. https://doi.org/10.1016/j.crad.2010.02.006
4. Yamamoto H, Oda Y (2015) Gastrointestinal stromal tumor: Recent advances in pathology and genetics. Pathol Int 65:9–18. https://doi.org/10.1111/pin.12230
5. Levy AD, Remotti HE, Thompson WM, et al (2003) Gastrointestinal stromal tumors: radiologic features with pathologic correlation. Radiographics 23:283–304. https://doi.org/10.1148/rg.232025146
6. Chavalitdhamrong D, Adler DG (2015) Complications of enteroscopy: how to avoid them and manage them when they arise. Gastrointest Endosc Clin North Am 25:83–95. https://doi.org/10.1016/j.giec.2014.09.002
7. Romano S, De Lutio E, Rollandi GA, et al (2005) Multidetector computed tomography enteroclysis (MDCT-E) with neutral enteral and IV contrast enhancement in tumor detection. Eur Radiol 15:1178–1183. https://doi.org/10.1007/s00330-005-2673-5
8. Soyer P, Aout M, Hoeffel C, et al (2013) Helical CT-enteroclysis in the detection of small-bowel tumours: A meta-analysis. Eur Radiol 23:388–399. https://doi.org/10.1007/s00330-012-2595-y

9. Vasconcelos RN, Dolan SG, Barlow JM, et al (2017) Impact of CT enterography on the diagnosis of small bowel gastrointestinal stromal tumors. Abdom Radiol 42:1365–1373. https://doi.org/10.1007/s00261-016-1033-z
10. Shinya T, Inai R, Tanaka T, et al (2017) Small bowel neoplasms: enhancement patterns and differentiation using post-contrast multiphasic multidetector CT. Abdom Radiol 42:794–801. https://doi.org/10.1007/s00261-016-0945-y
11. Foo WC, Liegl-Atzwanger B, Lazar AJ (2012) Pathology of gastrointestinal stromal tumors. Clin Med Insights Pathol 23–33. https://doi.org/10.4137/cpath.s9689
12. Fletcher CDM, Berman JJ, Corless C, et al (2002) Diagnosis of gastrointestinal stromal tumors: A consensus approach. Hum Pathol 33:459–465. https://doi.org/10.1053/hupa.2002.123545
13. Joensuu H (2008) Risk stratification of patients diagnosed with gastrointestinal stromal tumor. Hum Pathol 39:1411–1419. https://doi.org/10.1016/j.humpath.2008.06.025
14. Miettinen M Lasota J (2006) Gastrointestinal stromal tumors: pathology and prognosis at different sites. Semin Diagn Pathol 23:70–83. https://doi.org/10.1053/j.semdp.2006.09.001
15. Zhou C, Duan X, Zhang X, et al (2016) Predictive features of CT for risk stratifications in patients with primary gastrointestinal stromal tumour. Eur Radiol 26:3086–3093. https://doi.org/10.1007/s00330-015-4172-7
16. Bano S, Puri SK, Upreti L, et al (2012) Gastrointestinal stromal tumors (GISTs): An imaging perspective. Jpn J Radiol 30:105–115. https://doi.org/10.1007/s11604-011-0020-0
17. Burkill GJC, Badran M, Al-Muderis O, et al (2003) Malignant Gastrointestinal Stromal Tumor: Distribution, Imaging Features, and Pattern of Metastatic Spread. Radiology 226:527–532. https://doi.org/10.1148/radiol.2262011880
18. Ulusan S, Koc Z, Kayaselcuk F (2008) Gastrointestinal stromal tumours: CT findings. Br J Radiol 81:618–23. https://doi.org/10.1259/bjr/90134736
19. Shinagare AB, Ip IK, Lacson R, Ramaiya NH, George S KR (2015) Gastrointestinal Stromal Tumor : Optimizing the Use of Cross-sectional. Radiology 274:395–404. https://doi.org/10.1148/radiol.14132456
20. DeMatteo RP, Lewis JJ, Leung D, et al (2000) Two hundred gastrointestinal stromal tumors: recurrence patterns and prognostic factors for survival. Ann Surg 231:51–8. https://doi.org/10.1097/00000658-200001000-00008
21. Teoh WC, Teo SY, Ong CL (2011) Gastrointestinal stromal tumors presenting as gynecological masses: Usefulness of multidetector computed tomography. Ultrasound Obstet Gynecol 37:107–109. https://doi.org/10.1002/uog.8801
22. Cai PQ, Lv XF, Tian L, et al (2015) CT characterization of duodenal gastrointestinal stromal tumors. Am J Roentgenol. https://doi.org/10.2214/ajr.14.12870
23. Jinzaki M, Tanimoto A, Mukai M, et al (2000) Double-phase helical CT of small renal parenchymal neoplasms: Correlation with pathologic findings and tumor angiogenesis. J Comput Assist Tomogr 24:835–842. https://doi.org/10.1097/00004728-200011000-00002
24. Braschi-Amirfarzan M, Keraliya AR, Krajewski KM, et al (2016) Role of Imaging in Management of Desmoid-type Fibromatosis: A Primer for Radiologists. RadioGraphics 36:762–782. https://doi.org/10.1148/rg.2016150153
25. Cai PQ, Wu YP, Xie CM, et al (2013) Hepatic angiomyolipoma: CT and MR imaging findings with clinical-pathologic comparison. Abdom Imaging 38:482–489. https://doi.org/10.1007/s00261-012-9932-0
26. Lee SJ, Kim SY, Kim KW, et al (2016) Hepatic angiomyolipoma versus hepatocellular carcinoma in the noncirrhotic liver on gadoxetic acid-enhanced MRI: A diagnostic challenge. Am J Roentgenol 207:562–570. https://doi.org/10.2214/ajr.15.15602